Nanoscale

PAPER

View Article Online
View Journal | View Issue

Cite this: *Nanoscale*, 2014, **6**, 3150

Facile synthesis of boronic acid-functionalized magnetic carbon nanotubes for highly specific enrichment of glycopeptides†

Rongna Ma,[a] Junjie Hu,[a] Zongwei Cai[b] and Huangxian Ju*[a]

Received 9th October 2013
Accepted 27th November 2013

DOI: 10.1039/c3nr05367a

www.rsc.org/nanoscale

A stepwise strategy was developed to synthesize boronic acid functionalized magnetic carbon nanotubes (MCNTs) for highly specific enrichment of glycopeptides. The MCNTs were synthesized by a solvothermal reaction of Fe^{3+} loaded on the acid-treated CNTs and modified with 1-pyrenebutanoic acid *N*-hydroxysuccinimidyl ester (PASE) to bind aminophenylboronic acid (APBA) *via* an amide reaction. The introduction of PASE could bridge the MCNT and APBA, suppress the nonspecific adsorption and reduce the steric hindrance among the bound molecules. Due to the excellent structure of the MCNTs, the functionalization of PASE and then APBA on MCNTs was quite simple, specific and effective. The glycopeptides enrichment and separation with a magnetic field could be achieved by their reversible covalent binding with the boronic group of APBA–MCNTs. The exceptionally large specific surface area and the high density of boronic acid groups of APBA–MCNTs resulted in rapid and highly efficient enrichment of glycopeptides, even in the presence of large amounts of interfering nonglycopeptides. The functional MCNTs possessed high selectivity for enrichment of 21 glycopeptides from the digest of horseradish peroxidase demonstrated by MALDI-TOF mass spectrometric analysis showing more glycopeptides detected than the usual 9 glycopeptides with commercially available APBA–agarose. The proposed system showed better specificity for glycopeptides even in the presence of non-glycopeptides with 50 times higher concentration. The boronic acid functionalized MCNTs provide a promising selective enrichment platform for precise glycoproteomic analysis.

Introduction

Glycosylation, as one of the most important post-translational modifications of protein, plays key roles in a variety of biological activities, such as cell division, tumor immunology, inflammation, and so on.[1–4] It is essential to discover and identify the structures of glycopeptides or glycoproteins in diagnosis and proteomics. Mass spectrometry (MS) has been proven to be particularly useful for the analysis of protein glycosylation, especially for illuminating glycosylation-site occupancy and glycan heterogeneity at each glycosite.[5–8] However, the low abundance of glycopeptides and their poor ionization efficiency often results in signal suppression during mass spectrometric analysis.[9] Therefore, efficient methods of isolation and enrichment of glycopeptides/glycoproteins are indispensable in order to obtain an in-depth understanding of glycoproteomics.

Usually, glyco-specific enrichment can be achieved with lectin affinity chromatography,[10–13] size exclusion chromatography,[14,15] hydrazide chemistry[16–18] and hydrophilic interaction chromatography.[19–21] Recently, the boronate-functionalized matrix has gained increasing popularity for convenient enrichment of glycopeptides, since it is well known that diboronic groups bind with glycans and glycoconjugates containing *cis*-diol groups through reversible ester formation.[22–33] To date, several boronate-functionalized materials involving mesoporous silica,[25] polymer nanoparticles,[27] agarose resin[28] and magnetic nanoparticles[23,29–33] have been reported for the enrichment of glycopeptides. However, the functionalization process often suffers from harsh conditions (non-aqueous solvent, high temperature, *etc.*), multi-step reaction or cross-reactivity with other functional groups. Therefore, it is highly desirable to develop a facile strategy with mild conditions for the synthesis of boronate-functionalized materials, so that these materials can show better performance for selective enrichment of glycopeptides and glycoproteins.

Due to the outstanding mechanical, thermal and electrical properties, carbon nanotubes (CNTs) have been extensively utilized in different fields, including analytical and biomedical sciences.[34–40] Especially, aromatic molecules, such as pyrene, porphyrin and their derivatives, can interact with the CNTs sidewalls through π–π stacking interactions, providing an

[a]*State Key Laboratory of Analytical Chemistry for Life Science, School of Chemistry and Chemical Engineering, Nanjing University, Nanjing 210093, P.R. China. E-mail: hxju@nju.edu.cn; Fax: +86 25 83593593; Tel: +86 25 83593593*

[b]*Department of Chemistry, Hong Kong Baptist University, Kowloon Tong, Kowloon, Hong Kong SAR, P.R. China*

† Electronic supplementary information (ESI) available: EDX spectra, MALDI-TOF MS and data summary. See DOI: 10.1039/c3nr05367a

attractive approach for noncovalent functionalization to obtain controllable specificity.[36] Recently, graphene oxide has been reported to immobilize 1-pyrenebutyryl chloride for glycan enrichment.[41] This work designed a stepwise strategy to synthesize boronic acid functionalized magnetic carbon nanotubes (MCNTs) for highly specific enrichment and separation of glycopeptides (Scheme 1). The MCNTs were synthesized by a solvothermal reaction after Fe^{3+} was loaded on to acid-treated CNTs. The functionalization was performed by the adsorption of 1-pyrenebutanoic acid *N*-hydroxysuccinimidyl ester (PASE) on the surface *via* π–π stacking to bind aminophenylboronic acid (APBA) (Scheme 1A). The glycopeptide capture and release for the following MALDI-TOF MS analysis were achieved by reversible covalent binding of the boronic group with the hydroxyl groups of glycopeptides (Scheme 1B). The APBA–MCNTs showed high selectivity for enrichment of 21 glycopeptides in horseradish peroxidase (HRP) digests. The detectable concentration of the HRP digest was as low as 0.1 ng μL^{-1}. The excellent performance suggested that boronic acid functionalized MCNTs expand the application of carbon-based composites in the selective enrichment and separation of glycopeptides for further glycoproteome analysis.

Experimental

Materials and reagents

HRP (MW ~ 44 kDa), bovine serum albumin (BSA, MW ~ 66 kDa), asialofetuin (AF), lysozyme, PASE, 3-aminophenylboronic acid monohydrate (98%), FITC dye, ammonium bicarbonate (NH_4HCO_3), DL-dithiothreitol (DTT), iodoacetamide (IAA), trifluoroacetic acid (TFA, ≥90%) and α-cyano-4-hydroxycinnamic acid (CHCA) were purchased from Sigma-Aldrich (USA). Sequencing grade modified trypsin was obtained from Promega (Madison, USA). Acetonitrile (ACN) was obtained from Merck (Darmstadt, Germany). Iron(III) chloride hexahydrate ($FeCl_3 \cdot 6H_2O$), anhydrous sodium acetate (NaAc), ethylene glycol were purchased from Nanjing Chemical Reagent Co., Ltd. 1,6-Hexanediamine was purchased from Alfa (U.S.A), Carbon Nanotubes (CVD method, purity ≥98%, multiwalled, diameter 40–60 nm, and length 1–2 μm) were purchased from Nanoport Co. Ltd. (Shenzhen, China). All these reagents were used as received without further purification. Deionized water was prepared with a Milli-Q water purification system (Millipore, Milford, MA).

FITC-tagged protein was prepared by adding 50 μL FITC (1 mg mL^{-1} in DMSO) to 1 mL protein solution (5 mg mL^{-1}) in sodium carbonate buffer (0.1 M, pH = 9).

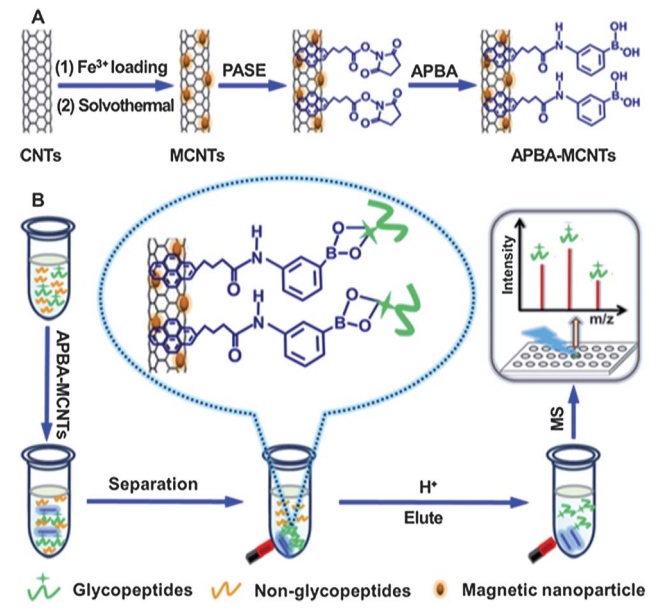

Scheme 1 Schematic illustration of (A) preparation of APBA–MCNTs and (B) specific enrichment and MS analysis of glycopeptides.

Apparatus

Scanning electron microscopic (SEM) images were obtained with a Hitachi S-3000N scanning electron microscope at an acceleration voltage of 10 kV. Transmission electron micrograph (TEM) was obtained on a JEM-2100 TEM (JEOL, Japan). Raman spectra were recorded using a Renishaw invia-Reflex Raman microscope system (Renishaw, UK). The magnetic property was measured using a superconducting quantum interference device (SQUID) at room temperature (RT). Powder X-ray diffraction patterns were recorded on Rigaku Dmax 2200 X-ray diffractometer (XRD) with Cu Kα radiation ($\lambda = 1.5416$ A). X-ray photoelectron spectroscopic (XPS) measurements were performed with an ESCALAB 250 spectrometer (Thermo-VG Scientific, USA) with an ultrahigh vacuum generator. Infrared spectra were obtained on a Nicolet NEXUS870 Fourier transform infrared (FT-IR) spectrometer (Madison, WI). The UV-vis absorption spectra were obtained with a UV-3600 UV-vis-NIR spectrophotometer (Shimadzu Co., Kyoto, Japan).

Preparation and boronic acid functionalization of MCNTs

MCNTs were synthesized with a solvothermal method.[42] CNTs were firstly sonicated with 3 : 1 (v/v) concentrated H_2SO_4–HNO_3 for 4 h to obtain the acid-treated CNTs. 50 mg of acid-treated CNTs were then dissolved in 5 mL of $FeCl_3$ solution (0.1 M) by sonication 1 h, followed by a 2 h shaking to load Fe^{3+} on CNTs, centrifugation, collection and drying at 60 °C overnight under vacuum. Afterwards the Fe^{3+} loaded CNTs were mixed with 12.5 mL of ethylene glycol, 1.2 g of NaAc and 0.375 g of 1,6-diaminohexane to perform the solvothermal reaction at 200 °C for 8 h. With a magnetic separation technique, the MCNT product was alternately washed with water and ethanol thrice, and vacuum-dried at 60 °C overnight.

Boronic acid-functionalized MCNTs were prepared through thrice repeated adsorption of PASE on MCNTs by mixing 1 mg MCNTs with 1 mL of 1 mM PASE in methanol with vibration for 60 min followed by magnetic separation, and reaction with 1 mL of 10 mM APBA and sonicated for 2 h. The as-prepared APBA–MCNTs were alternately washed with ethanol and water thrice, redispersed in water and stored in a refrigerator at 4 °C.

Adsorption capacity of proteins

The capacity of APBA–MCNTs for capture of glycoproteins or nonglycoproteins was identified by incubating 1 mg

APBA–MCNTs in 1 mL protein solution (in 20 mM pH 9.0 PBS) with a fixed concentration at room temperature (RT) overnight, and then the APBA–MCNTs were removed with an external magnetic field to determine the protein concentration in the remaining supernatant using a UV/Vis spectrophotometer. The adsorption capacity (Q) is calculated using eqn (1):

$$Q = (C_o - C_t) \times 10^3 \text{ (mg g}^{-1}\text{)} \quad (1)$$

where C_o (mg mL^{-1}) is the initial concentration of protein solution, C_t (mg mL^{-1}) is protein concentration in the remaining supernatant.

Digestion of proteins

After HRP or AF was dissolved in NH_4HCO_3 (50 mM, pH 8.3) to a final concentration of 1 mg mL^{-1}, and denatured at 100 °C for 5 min, trypsin was added in the solution at an enzyme-to-protein ratio of 1 : 40 (w/w) to digest the protein by incubation at 37 °C for 16 h. The digestion of BSA was performed by incubating a mixture of 50 μL of 200 mM DTT and 1 mL of 3 mg mL^{-1} BSA in 50 mM NH_4HCO_3 solution (pH 8.3) at 100 °C for 5 min, mixing the cooled solution with 40 μL of 1.0 M IAA at RT in the dark for 45 min, and adding trypsin in the mixture at an enzyme-to-protein ratio of 1 : 40 (w/w) for 16 h at 37 °C after the excessive IAA had been consumed with 200 μL of 200 mM DTT at RT for 1 h. All the tryptic peptide mixtures were stored at −20 °C until use.

Glycopeptide enrichment

After the digestion product was diluted with 50 mM NH_4HCO_3, 200 μL of APBA–MCNTs (1 mg mL^{-1}) was added into 500 μL of the diluted digestion product to incubate at RT with shaking for 2 h, it was then collected and washed three times with the same NH_4HCO_3 buffer to remove the nonspecifically adsorbed peptides with aid of an external magnetic field. The glycopeptide release was performed using ACN/H_2O/TFA (50 : 49 : 1, v/v/v; 50 μL) at RT for 1 h.

MALDI-TOF MS analysis

MALDI-TOF MS experiments were performed on a 4800 Proteomics Analyzer (Applied Biosystems, USA) equipped with the Nd-YAG laser at 355 nm, a repetition rate of 200 Hz and an acceleration voltage of 20 kV. After 1 μL of the eluate was deposited on a MALDI plate, 1 μL of saturated CHCA in 60% ACN (v/v) containing 1% TFA was introduced as a matrix to perform the MALDI-TOF MS analysis.

Results and discussion

Characterization of MCNTs and APBA–MCNTs

The SEM and TEM images of acid-pretreated CNTs displayed a uniform structure in the form of single tubes or small bundles with diameters of 40–60 nm (Fig. 1A and C), while the MCNTs showed obvious nanoparticles uniformly distributed on the walls of CNTs with the diameter of 10–15 nm (Fig. 1B and D). These nanoparticles were demonstrated to be Fe_3O_4 by the energy-dispersive X-ray spectra (Fig. S1†) and XRD patterns (Fig. 2A).

After loading Fe^{3+} and the solvothermal reaction, the XRD pattern showed some representative peaks of magnetite (JCPDS file no. 19-0629) at 2θ of 30.24°, 35.54°, 43.23°, 57.38° and 63.04° (Fig. 2A, curve b), different from the diffraction peaks at 26.02° and 43.14° occurring on the XRD pattern of acid-pretreated CNTs (Fig. 2A, curve a) for the graphite (002) and (100) planes of the CNTs, suggesting the presence of a magnetic phase in the MCNTs. The unchanged characteristic peaks of CNTs indicated that MCNTs remained in the original graphitic structure after the solvothermal reaction, which was further verified by Raman spectroscopy. The Raman spectra of both CNTs and MCNTs exhibited an active tangential mode peak (G band) around 1592 cm^{-1} corresponding to sp^2 hybridized carbon and the defect-induced mode peak (D band) around 1341 cm^{-1} originating from disordered carbon (Fig. 2B). The graphitic structure ensured the further functionalization of MCNTs *via* π–π stacking interaction.

The synthesized MCNTs showed the magnetic properties with a saturation magnetization value of 58.45 emu g^{-1} (Fig. 3, curve a) due to the presence of Fe_3O_4 nanoparticles, leading to a rapid response to the applied magnetic field (inset in Fig. 3). The value of saturation magnetization for APBA–MCNTs became 42.14 emu g^{-1} (Fig. 3, curve b), a little lower than that of MCNTs due to the surface chemical modification. Nevertheless, the relatively large saturation magnetization value was sufficient to accomplish fast and efficient separation with an external magnet, which was an advantage for their application.

The modification of MCNTs with APBA could be confirmed with FT-IR and XPS spectra (Fig. 4). The FT-IR spectrum of acid-treated CNTs showed a broad absorption band around 3400 cm^{-1} and a peak at 1640 cm^{-1}, assigned to the surface hydroxyl (O–H) bending and stretching modes of CNTs, respectively, a C=O stretching vibration band around 1700 cm^{-1} and a C–O–C stretching vibration band around 1100 cm^{-1} (Fig. 4A, curve a). These absorption bands indicated the presence of a carboxylic group. The FT-IR spectrum of MCNTs showed the strong IR band at 585 cm^{-1} (Fig. 4A, curve b), which is characteristic of Fe–O vibrations. The successful functionalization of MCNTs with APBA was clearly evidenced by the presence of the B–O

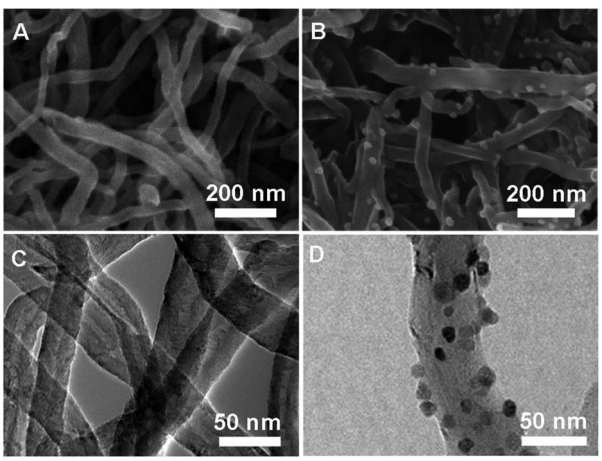

Fig. 1 (A and B) SEM and (C and D) TEM images of CNTs and MCNTs.

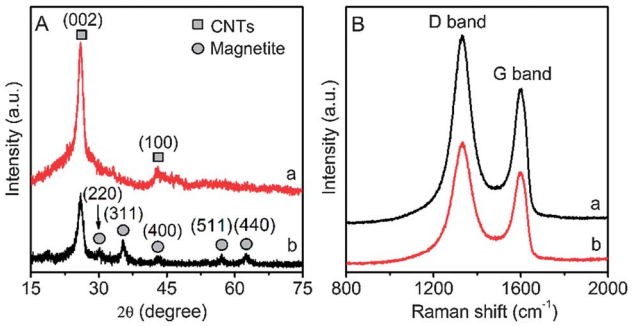

Fig. 2 (A) XRD patterns and (B) Raman spectra of (a) CNTs and MCNTs (b).

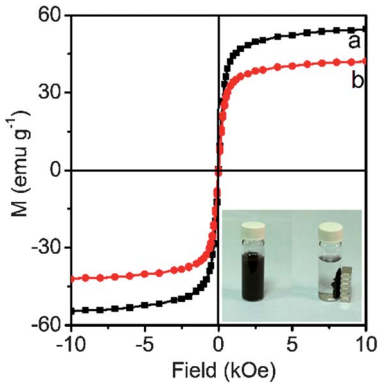

Fig. 3 Room-temperature magnetization curves of MCNTs (a) and APBA–MCNTs (b). Inset shows magnetic response of MCNTs to a magnet.

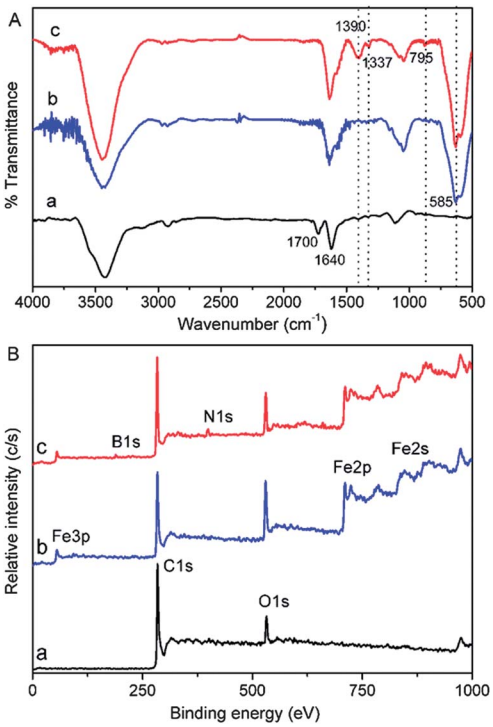

Fig. 4 (A) FT-IR and (B) XPS survey spectra of CNTs (a), MCNTs (b) and APBA–MCNTs (c).

adsorption at 1337 and 1390 cm^{-1}, and benzene ring vibration at 795 cm^{-1} (Fig. 4A, curve c).

The survey XPS spectrum of CNTs exhibited the C1s and O1s peaks at the binding energies of 284.8 and 531.4 eV, respectively (Fig. 4B, curve a), while the MCNTs showed the Fe signals at about 54.7 eV for Fe3p, 710.2 and 724.2 eV for Fe2p (Fig. 4B, curve b). After functionalization with APBA assisted by PASE, the survey XPS spectrum exhibited two new peaks of B1s and N1s at the binding energies of 188.6 and 398.5 eV, respectively (Fig. 4B, curve c). Although the signal of the B peak at 188.6 eV was relatively weak due to its low abundance, these results proved the successful binding of APBA to MCNTs.

Protein capture with APBA–MCNTs

The efficient capture of glycoprotein on APBA–MCNTs was confirmed using HRP as a model glycoprotein with confocal laser microscopy. The differences between the glycoprotein HRP and non-glycoproteins, lysozyme and BSA, could be clearly distinguished (Fig. 5A–E). FITC-tagged HRP showed strong fluorescence, while both FITC-tagged lysozyme and FITC-tagged BSA hardly showed any fluorescence signal on the APBA–MCNTs, indicating the high specificity of APBA–MCNTs for the capture of HRP. Moreover, the adsorption capacity measurements of APBA–MCNTs toward glycoproteins and non-glycoproteins, identified in the UV/Vis spectrum at different concentrations of protein, showed similar results. The maximum adsorption capacity of glycoproteins HRP was about 346 mg g^{-1}, which was much larger than 52 and 24 mg g^{-1} for BSA and lysozyme, respectively (Fig. 5F), which could be attributed to the specific binding between glycoproteins and phenylboronic acid *via* reversible ester formation.

Specific enrichment of glycopeptides

The specific recognition of APBA–MCNTs to glycopeptides was based on a typical borate esterification reaction, in which the boronic group reacted with *cis*-diols of glycan to form a

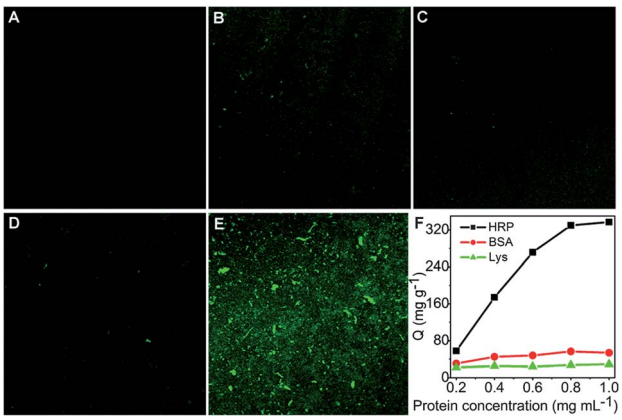

Fig. 5 Confocal images of (A) APBA–MCNTs, (B) MCNTs incubated with FITC-tagged HRP, and (C–E) APBA–MCNTs incubated with FITC-tagged lysozyme, BSA and HRP, respectively. (F) Adsorption isotherm of HRP, BSA and lysozyme on APBA–MCNTs.

heterocyclic diester in alkaline solution, and the esters dissociated on switching the medium to acidic pH. Due to the unique characteristics of the synthesized APBA–MCNTs, the selective enrichment capacity toward glycopeptides in the tryptic digest of HRP was examined by MALDI-TOF mass spectra. The direct analysis of HRP digest without enrichment showed only 7 peaks belonging to glycopeptides (labelled with H6, H15, H16, H17, H18, H19 and H21, respectively) due to the suppression of many dominant peaks of non-glycopeptides that were more abundant in the mixture (Fig. 6A). After enrichment with APBA–MCNTs, the additional 14 glycosylated peptides could be identified except for these mentioned 7 glycopeptides. The number of glycopeptides detected exceeded those of the previously reported boronic acid-functionalized mesoporous silica (5),[25] boronic acid-functionalized core–shell polymer nanoparticles (18)[27] and boronic acid-functionalized core-satellite composite nanoparticles (17)[29] for HRP digest enrichment, which can be attributed to the enhanced amount of boronic acid grafted onto MCNTs. Moreover, the most abundant non-glycosylated peptides existing in the HRP digest could be efficiently removed, and the signal-to-noise (*S*/*N*) ratio of the glycopeptides was obviously enhanced (Fig. 6B), suggesting excellent specificity of the APBA–MCNTs toward glycopeptides. The detailed sequence information is listed in Table S1 (ESI†).

To demonstrate the superiority of APBA–MCNTs for enrichment of glycopeptides, MCNTs and commercial APBA–agarose were used as a comparison. After enrichment with MCNTs, the HRP digest showed only 7 weak peaks assigned to glycopeptides (Fig. 6C), indicating that the APBA made a great contribution to the selective enrichment. However, the capture of glycopeptides in the same HRP digest with commercial APBA–agarose showed only 9 glycopeptides (Fig. 6D), much lower than the number detected upon enrichment with APBA–MCNTs. This can be attributed to the introduction of PASE, which reduced the steric hindrance, the excellent structure of MCNTs, the exceptionally large specific surface area and the high density of boronic acid groups of APBA–MCNTs. Therefore, the synergism of highly specific binding of APBA and high specific area of MCNT was the key factor for obtaining the excellent selectivity and sensitivity.

The sensitivity was examined with different concentrations of the HRP tryptic digest. In the digest of 0.1 ng μL^{-1} HRP, 10 glycopeptide peaks could be observed after enrichment with APBA–MCNTs (Fig. 7). The reason that some peaks observed in 10 ng μL^{-1} disappeared in this spectrum may be due to the much lower concentration of tryptic HRP digestion employed in this experiment. The detection limit was comparable with the previously reported boronic acid-functionalized core-satellite composite nanoparticles (0.1 ng μL^{-1})[29] and better than the boronic acid-functionalized core–shell polymer nanoparticles (1 ng μL^{-1}).[27] Meanwhile, the MALDI mass spectrum after enrichment with APBA–agarose could not give these glycopeptide signals when the concentration was increased by 10 times (Fig. S2, ESI†).

To further demonstrate the robustness of the designed enrichment material, the tryptic digest of AF, another glycoprotein, was examined. The direct analysis of AF digest without enrichment showed only 2 peaks of glycopeptides due to the overwhelming number of dominant peaks of non-glycopeptides (Fig. S3A†). After enrichment with APBA–MCNTs, 7 peaks assigned to diverse glycopeptides or their fragments were observed (Fig. S3B and Table S2 in the ESI†). The capture of glycopeptides in the same AF digest with commercial APBA–agarose showed only 3 glycopeptides (Fig. S3C†), much less than the number detected upon enrichment with APBA–MCNTs. Besides, the intensities and *S*/*N* of the peaks in Fig. S3C† were much lower than those in Fig. S3B.† These results demonstrated that the trap-and-release enrichment strategy was suitable for various glycopeptides. Moreover, compared with commercial APBA–agarose, the APBA–MCNTs had much stronger binding toward glycopeptides and could be used in the enrichment and analysis of glycopeptides at low concentration (Fig. S3E and F†).

The effect of highly abundant non-glycopeptides on the specific enrichment was further examined by mixing tryptic HRP and tryptic BSA in the mass ratios of 1 : 5, 1 : 10 and 1 : 50 (Fig. S4, ESI†). With the increasing amounts of tryptic BSA, the mass spectrometric responses of glycopeptides were not obviously suppressed by those of highly abundant non-glycosylated

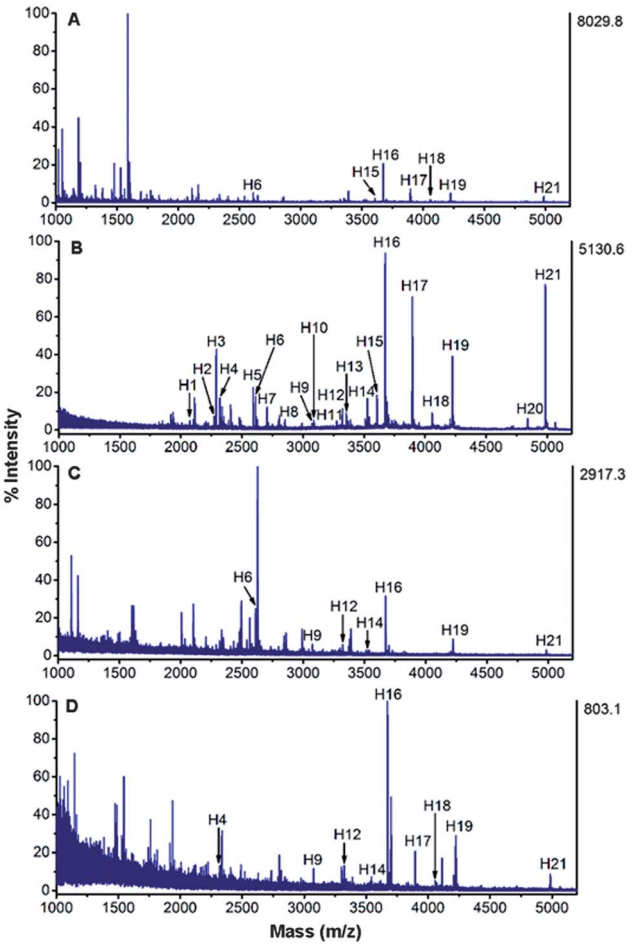

Fig. 6 MALDI mass spectra of tryptic digest of 5 ng μL^{-1} HRP (A) without and with enrichment by (B) APBA–MCNTs, (C) MCNTs and (D) commercial available APBA–agarose. The peaks of glycopeptides or their fragments are marked with H.

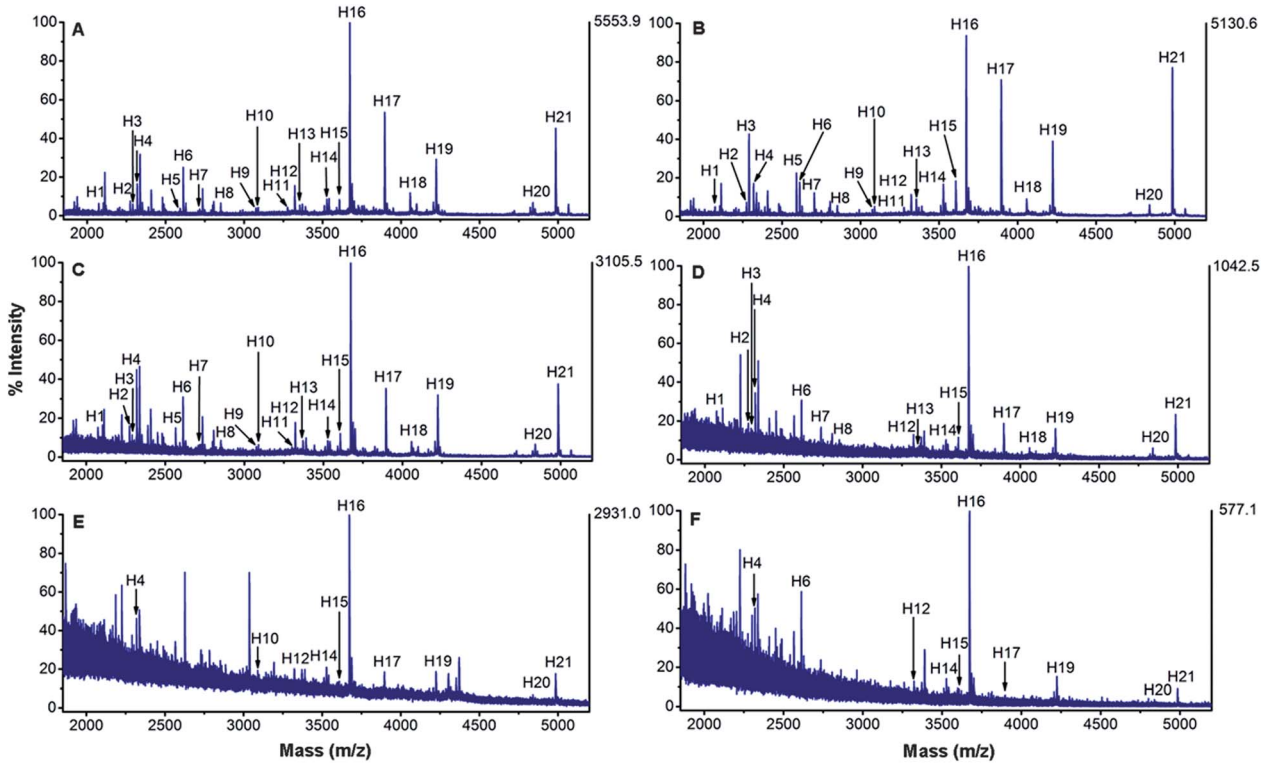

Fig. 7 MALDI mass spectra of tryptic digest of (A) 10, (B) 5, (C) 2, (D) 1, (E) 0.2 and (F) 0.1 ng μL^{-1} HRP after enrichment with APBA–MCNTs.

peptides. The APBA–MCNTs provided better specificity for glycopeptides, even when the non-glycopeptides were 50 times more abundant than the glycopeptides. Furthermore, the high-concentration salt and denaturants such as ammonium bicarbonate, dithiothreitol and iodoacetamide used in the process of BSA digestion did not affect the specific capture of glycopeptides. These results demonstrated the reliable performance of the APBA–MCNTs in the selective capture of glycopeptides from the complex substrate.

Conclusions

The MCNTs were successfully synthesized with a Fe^{3+}-involved solvothermal reaction and functionalized with APBA by a stepwise modification. The boronic group was introduced onto MCNTs by using PASE as a bridge for highly sensitive and selective enrichment of glycopeptides. The high saturation magnetization value of APBA–MCNTs simplified the separation of the glycopeptides from the sample. APBA–MCNTs possessed good dispersibility in aqueous solution, which greatly increased its binding rate and enrichment efficiency. The APBA–MCNTs could effectively capture 21 glycopeptides from HRP digests. The increased number and improved detection sensitivity for glycopeptides resulted from the synergism of highly specific binding of APBA and the high specific area of MCNT. The specific enrichment could exclude the suppression of highly abundant non-glycosylated peptides. In view of the ability to bind and concentrate many *cis*-diol molecules, the APBA–MCNTs should be a fascinating and promising material for high-throughput glycoproteome research in various fields.

Acknowledgements

This work was financially supported by the National Basic Research Program of China (2010CB732400) and National Natural Science Foundation of China (21121091, 21135002 and 91213301).

Notes and references

1 R. J. Woods, C. J. Edge and R. A. Dwek, *Nat. Struct. Mol. Biol.*, 1994, **1**, 499.
2 P. M. Rudd, T. Elliott, P. Cresswell, I. A. Wilson and R. A. Dwek, *Science*, 2001, **291**, 2370.
3 L. Wells, K. Vosseller and G. W. Hart, *Science*, 2001, **291**, 2376.
4 L. Lehle, S. Strahl and W. Tanner, *Angew. Chem., Int. Ed.*, 2006, **45**, 6802.
5 S. Pan, R. Chen, R. Aebersold and T. A. Brentnall, *Mol. Cell. Proteomics*, 2011, **10**, R110.003251.
6 H. Kaji, H. Saito, Y. Yamauchi, T. Shinkawa, M. Taoka, J. Hirabayashi, K.-i. Kasai, N. Takahashi and T. Isobe, *Nat. Biotechnol.*, 2003, **21**, 667.
7 Z. M. Segu, A. Hussein, M. V. Novotny and Y. Mechref, *J. Proteome Res.*, 2010, **9**, 3598.
8 W. Zhang, H. Wang, H. L. Tang and P. Y. Yang, *Anal. Chem.*, 2011, **83**, 4975.

9 A. Dell and H. R. Morris, *Science*, 2001, **291**, 2351.
10 E. H. Donnelly and I. J. Goldstein, *Biochem. J.*, 1970, **118**, 679.
11 R. D. Cummings and S. Kornfeld, *J. Biol. Chem.*, 1982, **257**, 1235.
12 J. Nawarak, S. Phutrakul and S. T. Chen, *J. Proteome Res.*, 2004, **3**, 383.
13 F. M. Okanda and Z. E. Rassi, *Electrophoresis*, 2006, **27**, 1020.
14 G. Alvarez-Manilla, J. Atwood, Y. Guo, N. L. Warren, R. Orlando and M. Pierce, *J. Proteome Res.*, 2006, **5**, 701.
15 D. F. Zielinska, F. Gnad, J. R. Wiśniewski and M. Mann, *Cell*, 2010, **141**, 897.
16 H. Zhang, X. J. Li, D. B. Martin and R. Aebersold, *Nat. Biotechnol.*, 2003, **21**, 660.
17 Y. Tian, Y. Zhou, S. Elliott, R. Aebersold and H. Zhang, *Nat. Protoc.*, 2007, **2**, 334.
18 Y. Li, Y. Tian, T. Rezai, A. Prakash, M. F. Lopez, D. W. Chan and H. Zhang, *Anal. Chem.*, 2011, **83**, 240.
19 Y. Wada, M. Tajiri and S. Yoshida, *Anal. Chem.*, 2004, **76**, 6560.
20 G. Palmisano, S. E. Lendal, K. Engholm-Keller, R. Leth-Larsen, B. L. Parker and M. R. Larsen, *Nat. Protoc.*, 2010, **5**, 1974.
21 M. H. J. Selman, M. Hemayatkar, A. M. Deelder and M. Wuhrer, *Anal. Chem.*, 2011, **83**, 2492.
22 J. H. Lee, Y. Kim, M. Y. Ha, E. K. Lee and J. Choo, *J. Am. Soc. Mass Spectrom.*, 2005, **16**, 1456.
23 W. Zhou, N. Yao, G. P. Yao, C. H. Deng, X. M. Zhang and P. Y. Yang, *Chem. Commun.*, 2008, 5577.
24 J. Tang, Y. C. Liu, D. W. Qi, G. P. Yao, C. H. Deng and X. M. Zhang, *Proteomics*, 2009, **9**, 5046.
25 Y. W. Xu, Z. X. Wu, L. J. Zhang, H. J. Lu, P. Y. Yang, P. A. Webley and D. Y. Zhao, *Anal. Chem.*, 2009, **81**, 503.
26 Z. Lin, J. N. Zheng, Z. W. Xia, H. H. Yang, L. Zhang and G. N. Chen, *RSC Adv.*, 2012, **2**, 5062.
27 Y. Y. Qu, J. X. Liu, K. G. Yang, Z. Liang, L. H. Zhang and Y. K. Zhang, *Chem.–Eur. J.*, 2012, **18**, 9056.
28 Q. B. Zhang, A. A. Schepmoes, J. W. C. Brock, S. Wu, R. J. Moore, S. O. Purvine, J. W. Baynes, R. D. Smith and T. O. Metz, *Anal. Chem.*, 2008, **80**, 9822.
29 L. J. Zhang, Y. W. Xu, H. L. Yao, L. Q. Xie, J. Yao, H. J. Lu and P. Y. Yang, *Chem.–Eur. J.*, 2009, **15**, 10158.
30 Z. A. Lin, J. N. Zheng, Z. W. Xia, H. H. Yang, L. Zhang and G. N. Chen, *RSC Adv.*, 2012, **2**, 5062.
31 X. H. Zhang, X. W. He, L. X. Chen and Y. K. Zhang, *J. Mater. Chem.*, 2012, **22**, 16520.
32 D. W. Qi, H. Y. Zhang, J. Tang, C. H. Deng and X. M. Zhang, *J. Phys. Chem. C*, 2010, **114**, 9221.
33 Z. C. Xiong, L. Zhao, F. J. Wang, J. Zhu, H. Q. Qin, R. A. Wu, W. B. Zhang and H. F. Zou, *Chem. Commun.*, 2012, **48**, 8138–8140.
34 A. Bianco, K. Kostarelos, C. D. Partidos and M. Prato, *Chem. Commun.*, 2005, 571.
35 C. Staii and A. T. Johnson, *Nano Lett.*, 2005, **5**, 1774.
36 R. J. Chen, Y. G. Zhang, D. W. Wang and H. J. Dai, *J. Am. Chem. Soc.*, 2001, **123**, 3838.
37 F. Balavoine, P. Schultz, C. Richard, V. Mallouh, T. W. Ebbesen and C. Mioskowski, *Angew. Chem., Int. Ed.*, 1999, **38**, 1912.
38 G. Lu, P. Maragakis and E. Kaxiras, *Nano Lett.*, 2005, **5**, 897.
39 B. Munge, G. D. Liu, G. Collins and J. Wang, *Anal. Chem.*, 2005, **77**, 4662.
40 K. Maehashi, T. Katsura, K. Kerman, Y. Takamura, K. Matsumoto and E. Tamiya, *Anal. Chem.*, 2007, **79**, 782.
41 W. J. Zhang, H. H. Han, H. H. Bai, W. Tong, Y. J. Zhang, W. T. Ying, W. J. Qin and X. H. Qian, *Anal. Chem.*, 2013, **85**, 2703.
42 Y. Zhang, Z. Y. Hu, H. Q. Qin, X. L. Wei, K. Cheng, F. J. Liu, R. A. Wu and H. F. Zou, *Anal. Chem.*, 2012, **84**, 10454.

